Electronic Supplementary Information for:

"Predicting surface anchoring: molecular organization across a thin film of 5CB liquid crystal on silicon"

A. Pizzirusso, R. Berardi, L. Muccioli, M. Ricci and C. Zannoni[♯]
Dipartimento di Chimica Fisica e Inorganica and INSTM,
Università di Bologna, Viale Risorgimento 4, 40136 Bologna, Italy

[♯] corresponding author e-mail: Claudio.Zannoni@unibo.it

Mesogen-Surface interaction

The intermolecular 5CB-surface interaction, calculated at the equilibrium B3LYP/6-31G* geometry for 5CB, is shown in Fig. ESI 1 for some significant approaching directions: either lying on the surface and parallel either to the (1,1) or (1-1) rows of surface hydrogens (or of the nano-grooves between them, Fig. ESI 1 a,b) or perpendicular to the surface with the cyano-group of 5CB pointing up or down (Fig. ESI 1 c,d). The interaction is quite strong: the potential well for a 5CB lying flat on the surface is significantly deeper than the side-side interaction between two 5CB molecules (∼40 kJ/mol [1]), while both energy minima are much larger than the room temperature $k_BT \sim 2.5$ kJ/mol, thus matching the conditions for a strong surface anchoring [2].

Anchoring energy

We employed a bottom up, molecular level approach for determining the anchoring energy as a function of molecular orientation on the surface by calculating an effective potential from the positional–orientational distribution function obtained from the simulation, scaled by the number of molecules $N(z)$ per unit surface area A as

$$W(z_i, \cos\beta) = -k_BT \ln P(z_i, \cos\beta)N(z_i)/A + W_0, \qquad (1)$$

where the subscript i indicates that z_i is a discrete variable, being the probability a histogram calculated from the simulation trajectory, z is the distance from the surface and β is the angle between the surface normal and the molecular long axis, W_0 is a constant used to shift the energy minimum to zero. From this free energy per unit area a fit can be performed with a Rapini-Papoular expression, minimizing the quantity $\chi(z)^2_{RP}$. The anchoring energy depends on the distance from the surface and a fit of the whole histogram is not physically meaningful, hence we performed it in 10 Å wide–intervals of

adjacent $M+1$ histogram bins centered on z and ranging from z_i to z_{i+M}. Also the sum in $\cos\beta$ is discrete but spans the whole range of this variable:

$$\chi^2_{RP}(z) = \sum_{j=i}^{j=i+M}\sum_{\cos\beta=-1}^{\cos\beta=+1} P(z_j,\cos\beta) \left\{W(z_j,\cos\beta) - [w_0^A(z) - \frac{1}{2}w_2^A(z)\sin^2(\beta-\beta_{eq}(z))]\right\}^2 . \quad (2)$$

For $\beta^d_{eq}(z)$ we employed the equilibrium director orientation at distance z (shown in Fig. 5 in the main text), and $w_0^A(z)$, $w_2^A(z)$ are the fitting parameters. Alternatively a generalized Rapini-Papoular expression can be used, minimizing the quantity $\chi^2_{GRP}(z)$:

$$\chi^2_{GRP}(z) = \sum_{j=i}^{j=i+M}\sum_{\cos\beta=-1}^{\cos\beta=+1} P(z_j,\cos\beta) \left\{W(z_j,\cos\beta) - [\sum_{L=0}^{4} u_L^A(z)P_L(\cos\beta)]\right\}^2 , \quad (3)$$

where P_L are the Legendre polynomials, and $u_L^A(z)$ the fitting parameters. In both cases each residual is weighted with the positional-orientational population $P(z_i,\cos\beta)$. The complete results of the fitting procedure for the two films at 300 and 315 K are given in Tables ESI 1 and ESI 2.

Molecular diffusion and instantaneous order parameter

A possible way of measuring the diffusion of particles from the first layer (the one in contact with the SiH surface) through the sample is to track their vertical position as a function of the time passed since they entered in that layer. In practice, we label particles as they enter the first layer, assumed to be 6 Å-thick, and follow their trajectory from this time on. We also record the maximum and minimum position as a function of time since they were tagged, as well as the percentage of particles still belonging to the first layer. This observable, unlike the persistence time, is able to tell us how far molecules diffuse throughout the sample since having entered the first layer, and how many of them are in it at certain time. Mobility is, as expected, higher in the isotropic phase and during the simulation time window molecules starting from the surface can travel up to ~ 160 Å away, compared to ~ 120 Å in the nematic phase, as shown in top and middle panels of Fig. ESI 2.

We also see (bottom panel of Fig. ESI 2) that the molecules in contact with the surface are still in fluid phase, in fact about 50% of the molecules which enter this region, then abandon it after 1 ns. However a fraction of molecules has much higher permanence times, as after 40 ns roughly 20% of particles still reside in the surface layer at both temperatures.
We recall here that the molecular dynamics at united atom level of modelling is faster because of the smoothing out of the molecular surface [3], so that absolute values of the permanence times are likely to be underestimated, but we expect the relative comparison to hold.

We report in Fig. ESI 3 the time evolution of the instantaneous order parameter P_{2L} for various layers L during the production runs. We point out that all the simulations were started from an isotropic phase and we have omitted plotting the equilibration runs. The limited diffusivity of LC molecules close to the surface is also accompanied by small fluctuations of their nematic order parameter P_{2L} during the simulation (blue lines labelled "layer 1" in Fig. ESI 3), which is observed in all samples, even in the isotropic phase. In the other sections of the films instead the fluctuations of P_{2L} are rather large, in particular in the center (black lines), and at the interface with vacuum (red lines). The absence of systematic drifts in the layers order parameters, and the fact that several oscillation periods are sampled, demonstrate that the configurations are well equilibrated, also on a local scale.

References

[1] G. Prampolini, *J. Chem. Theory Comput.*, 2006, **2**, 556.

[2] P. G. de Gennes and J. Prost, *The Physics of Liquid Crystals*, Oxford U. P., 1993.

[3] G. Tiberio, L. Muccioli, R. Berardi, and C. Zannoni, *ChemPhysChem*, 2009, **10**, 125–136.

Table ESI 1: Anchoring energies parameters at 300 K obtained by fitting 10 Å-wide portions of the energy distribution histogram $W(z, \cos\beta)$ with the Rapini-Papoular expression (w_0^A, w_2^A as in eq. 2) and a more general expression (u_0^A, u_1^A, u_2^A, u_3^A, u_4^A, eq. 3). Energies and mean square errors are reported in units of $10^{-2} J/m^2$. The equilibrium orientation of the local director β_{eq} has been evaluated from the local director of the layer (cf Fig. 5 in the main text) as $\beta_{eq} = \cos^{-1}(1 - n_z)$.

z (Å)	mols/Å^2	β_{eq}°	w_0^A	w_2^A	MSE	u_0^A	u_1^A	u_2^A	u_3^A	u_4^A	MSE
300 K (N=1000)											
5	0.0262	14	7.52	11.61	2.17	4.52	0.00	3.21	0.00	-3.49	1.55
15	0.0256	23	4.21	3.04	1.64	4.19	0.00	3.20	0.00	-0.30	0.31
25	0.0250	27	3.83	1.99	1.18	3.88	0.00	2.43	0.00	-0.14	0.12
35	0.0250	32	3.60	1.22	0.96	3.73	0.00	1.94	0.00	-0.09	0.09
45	0.0249	40	3.37	0.31	0.73	3.59	0.00	1.42	0.00	0.02	0.13
55	0.0249	51	3.30	0.32	0.39	3.48	-0.05	0.80	-0.04	0.14	0.10
65	0.0243	64	3.31	0.31	0.15	3.37	-0.12	0.09	-0.13	0.15	0.13
75	0.0258	77	3.85	1.82	0.27	3.58	-0.06	-0.84	0.00	0.21	0.11
85	0.0225	86	3.82	3.14	0.22	3.31	0.10	-1.05	-0.26	0.02	0.21
95	0.0272	90	6.43	10.46	0.97	4.79	-0.52	-3.48	0.21	0.03	0.87
105	0.0268	88	5.57	8.63	1.33	4.30	0.91	-2.59	-0.55	-0.34	1.13
115	0.0021	80	0.47	0.29	0.24	0.47	0.18	0.03	0.01	-0.01	0.21
300 K (N=2000)											
5	0.0263	13	8.19	12.93	2.11	4.42	0.00	2.73	0.00	-3.86	1.65
15	0.0255	22	4.31	3.24	1.76	4.27	0.00	3.41	0.00	-0.19	0.36
25	0.0251	27	3.89	2.06	1.24	3.95	0.00	2.57	0.00	-0.05	0.14
35	0.0251	28	3.79	1.77	1.15	3.89	0.00	2.38	0.00	-0.07	0.10
45	0.0250	29	3.75	1.64	1.12	3.86	0.00	2.31	0.00	0.02	0.10
55	0.0251	29	3.76	1.60	1.09	3.85	0.00	2.27	0.00	0.11	0.10
65	0.0250	29	3.72	1.54	1.13	3.86	0.00	2.34	0.00	0.11	0.10
75	0.0251	29	3.75	1.57	1.06	3.83	0.00	2.19	0.00	-0.01	0.09
85	0.0251	31	3.67	1.34	1.04	3.81	0.00	2.13	0.00	0.04	0.09
95	0.0250	33	3.56	1.05	1.03	3.78	0.00	2.05	0.00	0.05	0.09
105	0.0250	37	3.45	0.65	0.94	3.73	0.00	1.84	0.00	0.05	0.08
115	0.0250	42	3.35	0.17	0.82	3.67	-0.06	1.63	-0.03	0.20	0.08
125	0.0250	48	3.31	0.21	0.69	3.62	-0.03	1.38	0.01	0.40	0.08
135	0.0249	54	3.30	0.45	0.47	3.53	-0.07	0.93	-0.03	0.45	0.10
145	0.0251	60	3.37	0.42	0.26	3.50	-0.05	0.44	-0.02	0.52	0.08
155	0.0249	66	3.43	0.03	0.20	3.47	-0.04	0.02	-0.05	0.52	0.08
165	0.0250	72	3.57	0.70	0.25	3.50	-0.04	-0.43	-0.03	0.50	0.08
175	0.0246	78	3.76	1.93	0.35	3.52	-0.05	-0.95	-0.07	0.52	0.12
185	0.0259	82	4.35	4.01	0.48	3.87	-0.11	-1.82	0.02	0.59	0.12
195	0.0235	85	4.32	4.51	0.22	3.61	0.20	-1.66	-0.07	0.38	0.14
205	0.0254	87	5.46	8.21	1.16	4.42	-0.45	-3.03	0.00	0.22	0.83
215	0.0292	88	6.31	9.98	1.41	4.72	0.70	-3.22	-0.46	-0.07	1.35
225	0.0049	87	0.98	0.84	0.57	0.98	0.38	-0.02	0.01	0.00	0.46

Table ESI 2: Anchoring energies parameters at 315 K, see table ESI 1 for details.

z (Å)	mols/Å^2	β_{eq}°	w_0^A	w_2^A	MSE	u_0^A	u_1^A	u_2^A	u_3^A	u_4^A	MSE
315 K (N=1000)											
5	0.0256	15	7.01	10.49	2.31	4.51	0.00	3.52	-0.02	-2.91	1.56
15	0.0249	23	4.18	2.67	1.16	3.89	0.00	2.23	-0.04	-0.33	0.35
25	0.0244	32	3.63	0.91	0.62	3.60	0.00	1.28	-0.01	-0.10	0.12
35	0.0243	42	3.43	0.10	0.39	3.50	0.00	0.79	-0.07	-0.02	0.09
45	0.0243	52	3.38	0.24	0.19	3.46	0.00	0.41	-0.14	0.05	0.07
55	0.0243	62	3.42	0.14	0.07	3.45	-0.03	0.06	-0.25	0.05	0.06
65	0.0241	71	3.51	0.45	0.12	3.44	-0.04	-0.26	-0.10	0.05	0.07
75	0.0247	79	3.80	1.69	0.17	3.53	-0.05	-0.67	-0.01	0.04	0.07
85	0.0231	86	3.76	2.22	0.11	3.39	0.13	-0.72	-0.07	-0.01	0.11
95	0.0246	90	5.11	7.08	0.56	3.97	-0.40	-2.13	-0.14	-0.09	0.50
105	0.0289	89	6.34	9.98	0.90	4.74	0.53	-3.31	-0.30	0.03	0.84
115	0.0071	80	1.47	1.37	0.77	1.36	0.50	-0.12	-0.03	-0.02	0.65
315 K (N=2000)											
5	0.0255	19	5.79	8.09	2.34	4.44	0.00	3.44	0.00	-2.87	1.29
15	0.0250	28	3.86	1.88	1.16	3.83	0.00	2.08	0.00	-0.32	0.33
25	0.0244	36	3.51	0.58	0.60	3.57	0.00	1.19	0.00	-0.05	0.13
35	0.0243	42	3.43	0.13	0.35	3.49	0.00	0.73	0.00	-0.01	0.09
45	0.0243	47	3.40	0.10	0.21	3.46	0.00	0.43	0.00	-0.05	0.06
55	0.0243	50	3.40	0.11	0.15	3.44	0.00	0.29	0.00	-0.05	0.07
65	0.0243	51	3.41	0.10	0.13	3.45	0.00	0.26	0.00	-0.01	0.06
75	0.0242	51	3.40	0.08	0.17	3.44	0.00	0.34	0.00	-0.03	0.07
85	0.0242	51	3.38	0.15	0.19	3.45	0.00	0.40	0.00	-0.01	0.06
95	0.0243	50	3.40	0.12	0.16	3.45	0.00	0.32	0.00	0.01	0.06
105	0.0243	48	3.42	0.02	0.17	3.44	0.00	0.33	0.00	0.03	0.07
115	0.0243	48	3.42	0.03	0.18	3.45	0.00	0.37	-0.02	0.02	0.06
125	0.0243	48	3.42	0.02	0.17	3.45	0.01	0.34	0.00	-0.01	0.06
135	0.0242	49	3.39	0.10	0.17	3.44	-0.01	0.35	0.00	-0.05	0.06
145	0.0242	51	3.39	0.14	0.16	3.44	0.00	0.33	0.01	0.03	0.06
155	0.0242	55	3.39	0.15	0.12	3.43	-0.01	0.22	-0.03	0.03	0.06
165	0.0243	60	3.42	0.08	0.07	3.44	-0.01	0.04	0.00	0.03	0.06
175	0.0241	66	3.45	0.14	0.06	3.42	0.00	-0.07	-0.04	-0.02	0.06
185	0.0241	73	3.54	0.69	0.18	3.43	-0.09	-0.39	-0.02	-0.05	0.09
195	0.0248	80	3.88	2.07	0.15	3.54	0.04	-0.75	0.03	0.00	0.09
205	0.0221	85	3.85	3.30	0.29	3.32	-0.07	-1.04	-0.27	-0.15	0.27
215	0.0279	89	6.56	10.60	0.64	4.96	-0.39	-3.75	0.31	0.11	0.44
225	0.0219	88	4.40	6.23	1.17	3.59	0.89	-1.72	-0.36	-0.29	0.83
235	0.0008	82	0.20	0.06	0.08	0.21	0.06	0.03	0.00	-0.01	0.07

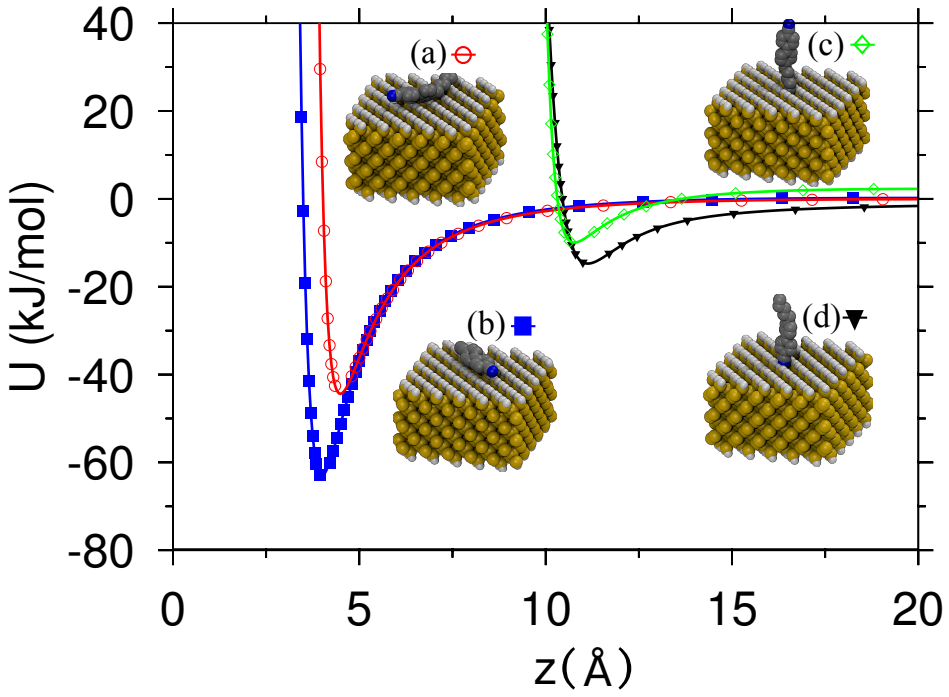

Figure ESI 1: Intermolecular energy of a surface–5CB system as function of distance from Si(001):H plane for selected orientations of 5CB (a-d) as shown.

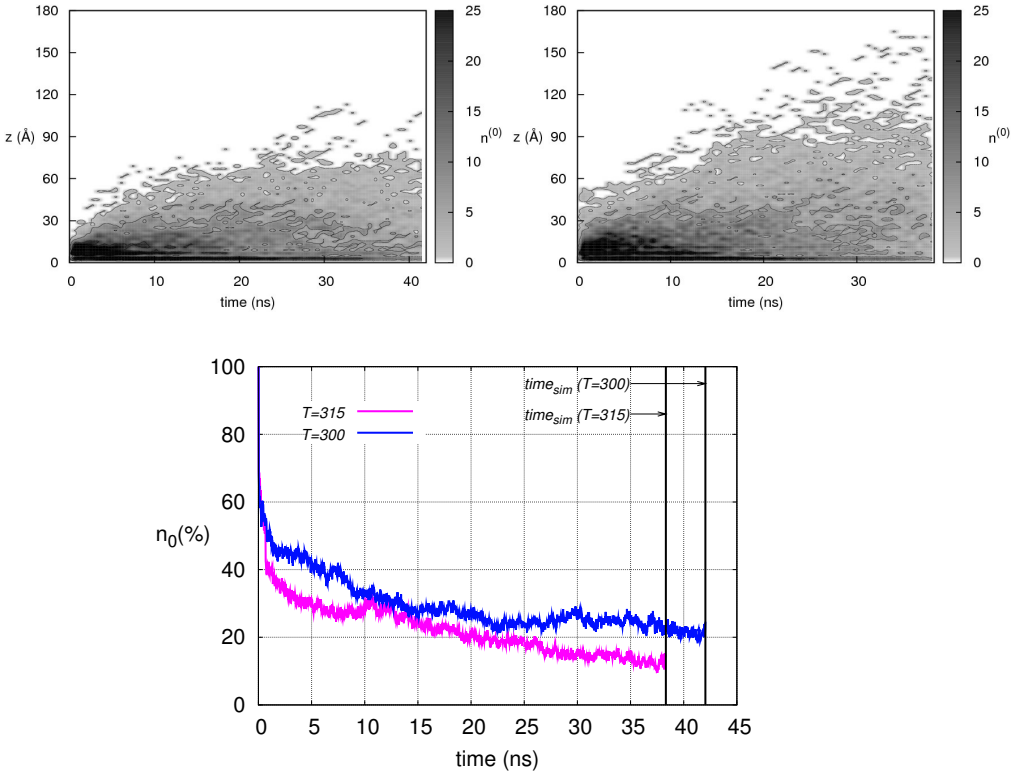

Figure ESI 2: Time–dependent distribution density of distances from the Si surface travelled by 5CB molecules after leaving the first 6 Å-thick overlayer. We show results at $T = 300$ K (top) and $T = 315$ K (central panel). On the bottom we show the percentage population of molecules still present in the first layer at a given time once their presence has been observed there.

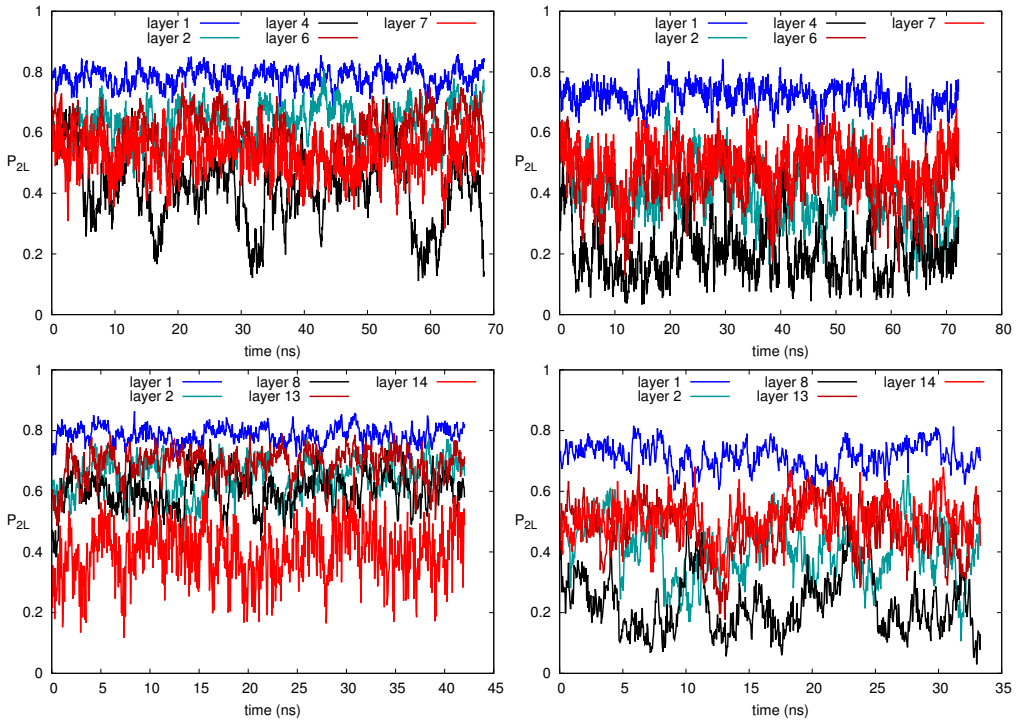

Figure ESI 3: Order parameter of 5CB versus simulation time for selected layers for the different samples: N=1000, T=300 K (top left), N=1000; T=315 K (top right); N=2000, T=300 K (bottom left); N=2000, T=315 K (bottom right). The labelling of the layers corresponds to the one used for figures 4 and 5 in the main text.